Future Journal of Pharmaceutical Sciences

RESEARCH

Open Access

The design and evaluation of ciprofloxacin-loaded nanoformulations using *Ipomoea batatas* starch nanoparticles

Tolulope O. Ajala[1], Omobolanle A. Omoteso[2*] and Oladotun M. Awe[1]

Abstract

Background Starch nanoparticle derivatives are gaining popularity as drug delivery vehicles because of their biocompatibility, better mechanical characteristics, heat stability properties, impediment qualities, permeability capabilities, and flexibility to be changed for specific predetermined functions. The effect of techniques and processing time on the physiochemical and drug release characteristics of sweet potato (Ipomoea batatas) starch nanoparticles and their ciprofloxacin-loaded nanoformulations was studied.

Results Scanning electron microscopy confirmed that the treated starch formed nanoparticles and also revealed significant changes in the morphology of the treated starches. The water absorption capacity of chemically treated starch nanoparticles (CTSN)-3 days was the highest, whereas CTSN-6 days had the maximum solubility. The functional groups present in the starch nanoparticles were confirmed by Fourier transform infrared spectroscopy and Raman. The thermal characteristics of starch nanoparticles were established using hot-stage microscopy, differential scanning calorimetry, and thermogravimetric analysis. The percentage drug content and loading efficiency of the model drug were extensively boosted by the chemical and mechanical treatment of *Ipomoea batatas* starch. In comparison with the untreated potato starch (UPS), release times for loaded drug were significantly longer for the chemically treated starch nanoparticles and mechanically treated starch nanoparticles (MTSN) starches in the rank order of $T_{80\%}$, CTSN-3 days > MTSN-3 days > CTSN-6 days > MTSN-6 days > UPS. The main kinetics of drug release were Fickian diffusion.

Conclusion After 3 days of acid hydrolysis, sweet potato starch yielded nanoparticulate carriers that can be employed for controlled or extended release of medicines that are poorly water soluble.

Keywords Starch nanoparticle, Acid hydrolysis, Mechanical treatment, Ipomoea batatas, Drug release studies

Background

Nanotechnology is the design and fabrication of systems at the atomic and molecular levels in order to manufacture objects as small as a few hundred nanometers. These systems are created by building each component from the top-down or bottom-up. The usage of nanotechnology in the delivery of drugs has altered the landscape of pharmaceutical and biotechnology firms [1–4]. Nanoshells, polymer conjugates, nanoparticles, dendrimers, micelles, carbon nanotubes, proteins, liposomes, and quantum dots are some examples of nanotechnology drug delivery methods used [1, 4].

Nanoparticles are colloidal particles with diameters spanning from 1 to 1000 nm; although several preferential sizes exist, they are employed for specific nanomedicine applications [1]. Nanoparticles manufactured from natural polymers have gained significant interest because (1) they can be modified for targeted drug

*Correspondence:
Omobolanle A. Omoteso
omotesoomobolanle@gmail.com
[1] Department of Pharmaceutics and Industrial Pharmacy, University of Ibadan, Ibadan, Nigeria
[2] School of Pharmacy, University of the Western Cape, Bellville, Cape Town 7530, South Africa

administration; (2) they improve solubility and bioavailability; (3) they serve as important carriers in the delivery of poorly soluble pharmaceuticals; and (4) they can control drug release from a single dose and prevent endogenous enzymes from degrading it [5].

Starch is a biopolymer that is naturally occurring, plentiful, and renewable. Its low cost, biodegradability, non-toxicity, and biocompatibility make it particularly appealing and of great interest in numerous nanoparticulate research fields [6, 7]. Many plants store starch as an energy source during photosynthesis. This polymer has glucose-based amylose and amylopectin granules. Starch is derived from a variety of plant types, including cereals or grains, roots, tubers, legumes, and fruits [4, 8, 9]. Because of its granules' poor solubility, weak reactive surface, high viscosity, and ability to create a cohesive paste, starch has limited utility in industry. Modifications can improve certain qualities and add more functional groups to starch [4, 10, 11].

Starch nanoparticles (SNPs) are particles with at least one dimension less than 1000 nm but greater than a single molecule or atom [10]. Starch nanoparticles are not the same as starch nanocrystals. Starch nanocrystals, also known as starch crystallite or microcrystallite, are crystalline or formed from the disruption of the amorphous domain of the semicrystalline structure of starch granules, whereas starch nanoparticles are amorphous and formed from gelatinized starch [12, 13].

Gallant et al. [14] and Tang et al. [15] found nano-sized semicrystalline blocklets in starch granules. Mild hydrolysis with acids or enzymes can extract nano-blocklets from starch. Physical therapy may potentially break down the starch granules, allowing the nano-blocklets to be released. These SNPs contain a crystalline moiety and the inherent advantages of starch granules, namely renewability and biodegradability [16]. SNPs can be produced through different types of methods, including chemical (acid hydrolysis), mechanical/physical (sonication, milling, thermosonication, spray-drying), enzymatic (enzyme debranching), and nano-precipitation, which convert the morphology of starch granules to nanoparticles [4, 6, 10]. When compared to native starch, starch nanoparticles exhibit distinct physiochemical and biological properties. This potential property includes better solubility, improved biological penetration rate, strong reactive surfaces, and increased absorption capacity, allowing them to be used as carriers and for the transportation of bioactive substances into impermeable anatomical regions instead of lipid micelles [10].

Ipomoea batatas (sweet potato) (Convolvulaceae family) is a perennial plant found in many warm temperate, subtropical, and tropical climates. Sweet potatoes are a high-starch food and medicinal ingredient. Sweet potato starch concentration ranges from 6 to 31%. Previous research has used Ipomoea batatas starch as a binder and disintegrant [17, 18]. Sweet potato was selected for the study for the following reasons. Potato is reported as one of the world's most versatile and under-exploited food crops with high nutritional value. The starch is preferred in the food and pharmaceutical industry because the paste has acceptable clarity due to the low amount of protein and lipids; in addition, the flavor is neutral unlike other starches [19].

Ciprofloxacin inhibits Gram-positive and Gram-negative bacteria. It treats lung, urinary, otitis media, and external ocular infections [20, 21]. Ciprofloxacin is classified as class 4 by the Biopharmaceutical Classification System, signifying low permeability and solubility, resulting in poor bioavailability as well as poor absorption and considerable variability [22]. Ciprofloxacin is available in tablet form and is administered twice a day at a dose of 500 mg. The use of starch nanoparticles in the delivery of ciprofloxacin is predicted to improve the drug's solubility, bioavailability, and cellular permeability, resulting in a dose or frequency of administration reduction. The goal of this work was to determine how different preparation methods and processing times affected the characteristics of Ipomoea batatas starch nanoparticles and their ciprofloxacin-loaded nanoformulations.

Materials and methods

Materials

Ipomoea batatas was sourced locally. The potato starch was prepared in the laboratory.

Methods

Extraction of Ipomoea batatas starch

Ipomoea batatas tubers were washed with distilled water, peeled, and wet-milled using a laboratory blender (Panasonic Mixer and Grinder MX-AC400). The slurry was sieved using a calico cloth to remove the chaff, and the filtrate was allowed to settle before being decanted. The starch sediment was constantly washed until the supernatant was colorless. The wet bulk was dried in a hot air oven (Gallenkamp BS Oven 250) at 50 °C for 48 h. The dried potato starch was mixed in a laboratory mill and screened through a 120 mesh sieve to produce a fine powder that was weighed and kept in sealed containers until needed [23].

Preparation of starch nanoparticles

Chemically treated starch nanoparticles (CTSN) SNPs were synthesized using the procedures published by Kim et al. [24], with minor modifications. 800 mL of 2.2 M hydrochloric acid was used to hydrolyze 40 g of untreated potato starch (UPS). A temperature-controlled

mechanical shaker was used to continually mix the suspension at 100 rpm at 40 °C. (Brunswick Scientific Incubator Shaker, Thermo Scientific, USA). Two batches were prepared by varying the incubation period for 3 and 6 days, respectively. After the experiments, successive washings were done to return the starch to its initial pH of 4. Following that, the starch nanoparticles were freeze-dried (Christ/Alpha 1–2 LD plus Dryer). For the mechanically treated starch nanoparticles (MTSN), the UPS suspensions were subjected to mechanical shaking and stirring at 100 rpm at 40 °C for 3 and 6 days, respectively, and then freeze-dried.

Water absorption capacity and solubility (WAC)

WAC was determined by adding distilled water (15 ml) to 2.5 g of USP, CTSN, and MTSN. The samples were vortexed for 2 min before being centrifuged at 400 rpm for 20 min. The supernatant was decanted, and the residue was weighed and dried to a constant weight in an oven. The WAC was then expressed as the weight of water bound to 100 g of each sample. Similarly, solubility was determined with 1 g (W) of sample in a conical flask and 15 ml of distilled water was added and agitated for 5 min. It was placed in a water bath and heated at 60 degrees for 20 min with constant stirring. It was put into a pre-weighed centrifuge tube ($W1$) and centrifuged for 20 min at 2200 rpm. The supernatant was decanted into a pre-weighed dish ($W2$), dried at 100 degrees to constant weight ($W3$), and cooled [25].

$$\text{Solubility}\,(\%) = \{(W2 - W3)/W\} \times 100$$

Preparation of ciprofloxacin-loaded starch nanoparticles

Ciprofloxacin (250 mg) was dissolved in 250 ml acetic acid (0.1 M). The treated or untreated potato starch (5 g) was then dispersed into the prepared solution of ciprofloxacin. The mixture was placed on a magnetic stirrer and rotated for 1 h. The mixture was centrifuged, decanted, and air-dried. A UV spectrophotometer was used to measure the quantity of drug in the supernatant. The following formulae were used to compute the drug content and loading efficiency [13]:

$$\text{Drug content}\,(\%) = \left(x/y\right) \times 100$$

where x = weight of the drug in the starch nanoparticle; y = weight of the starch nanoparticle.

$$\text{Loading efficiency}\,(\%) = (a/b) * 100$$

where a = weight of the drug in the starch nanoparticle; b = first weight of the drug in the loading solution.

Characterization of untreated potato starch (UPS), chemically treated starch nanoparticles (CTSN), and mechanically treated starch nanoparticles (MTSN)

Scanning electron microscopy (SEM)

The surface structure and particle size of the UPS and SNPs were determined utilizing SEM (JEOL, JSM-6060LV (Tokyo, Japan). Samples were placed on aluminum stubs and glazed with a gold film under a vacuum in a sputter coater. The observation was done at different magnifications.

Differential scanning calorimetry (DSC)

The samples' DSC thermograms were generated using a PerkinElmer DSC 8000. (Waltham, USA). These samples were prepared by precisely weighing around 2.5 g of each sample into an aluminum pan and completely closing it with an aluminum cover. Following that, heating from 25 °C (room temperature) to 400 °C at a pace of 10 °C/min in an inert nitrogen environment with a flow tempo of 20 ml/min. The reference was a covered, empty aluminum pan [26].

Thermogravimetric analysis (TGA)

The samples' TGA thermograms were determined using a Perkin Elmer TGA 4000. (Waltham, USA). In a porcelain crucible, about 3 mg sample was deposited. The sample was then heated from 30 °C up until 600 °C with a nitrogen purge of 20 ml/min and a heating speed of 10 °C/min [26].

Hot-stage microscopy (HSM)

The samples' HSM micrographs were obtained utilizing an Olympus optical (Japan) microscope with a LinkPad THMS600 heating stage (Linkam Scientific Instruments Ltd., Surrey, UK). Each sample was soaked in silicon oil and heated from ambient temperature (25 °C ± 2) at a speed of 10 °C/min until degradation was noticed. Using an Olympus UC30 camera and Stream Essentials software linked to the microscope, images were captured and temperatures were recorded at each detectable thermal change [26].

Fourier transform infrared spectroscopy (FTIR)

The samples' FTIR spectrograms were determined utilizing a Perkin Elmer Spectrum 400 spectrometer (Waltham, USA). The samples were placed on the equipment's already cleaned diamond crystal. For each sample, the analysis was performed at 650–4000 cm^{-1} with four scans at resolutions ranging from 2 to 4 cm^{-1}/s [26].

Raman spectroscopy

The samples' Raman spectrograms were produced using an Anton Paar Raman spectrophotometer. The samples were set in the equipment sampling chamber after being poured into small conical glass vials. The data were analyzed using a 1064 nm wavelength in the range of 0 to 2500 cm^{-1}.

In vitro release study of Ciprofloxacin-loaded starch nanoparticles

The release measurement in 900 ml buffer solution was conducted in a dissolution test apparatus using phosphate buffer of pH 6.8. The drug-loaded starch nanoparticles and drug-loaded untreated potato starch were packed into capsule shells. The buffer medium in the receptor vessels was maintained at 37 °C and rotated at 100 rpm. Approximately 5 ml of the receptor vessels' fluid were withdrawn at various predetermined durations (5, 10, 15, 30, 45, 60, 90, 120, and 150 min), and the percentage of the extract-mediated silver nanoparticles released was analyzed using UV–visible spectrophotometer at 315 nm. The sink method was maintained, through the replacement of 5 ml of the pure buffer solution after every sample withdraws from the vessels. The cumulative percentage drug released was calculated and plotted versus time [27].

Results

Figures 1, 2, 3, 4, 5, 6, 7, 8 and 9.

Discussion

As previously stated, starch nanoparticles (SNPs) are distinct from starch nanocrystals but are also referred to as starch nanocrystals (SNCs). The crystalline fraction of starch granules that remains following acid or enzymatic hydrolysis or other mechanical processes is referred to as SNCs. However, the word starch 'nanocrystals' refers to solely the crystalline section, while 'nanoparticles' can also encompass amorphous portions [28]. Starch can be modified to change its morphology by influencing

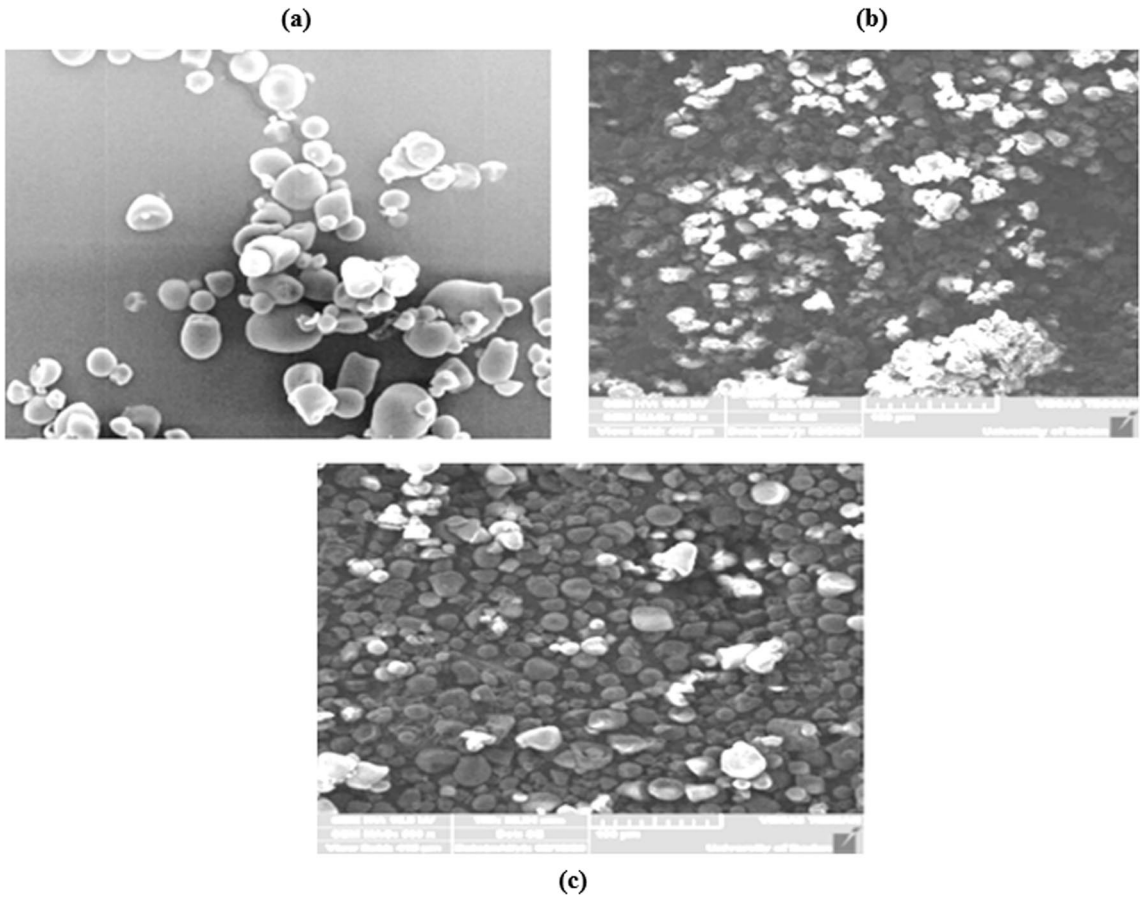

Fig. 1 SEM micrographs of **a** untreated potato starch, **b** chemically treated potato starch-6 days, and **c** mechanically treated potato starch-6 days. Scanning electron microscopy (SEM) photomicrographs of untreated potato starch, chemically treated starch nanoparticles-6 days, and mechanically treated starch nanoparticles-6 days

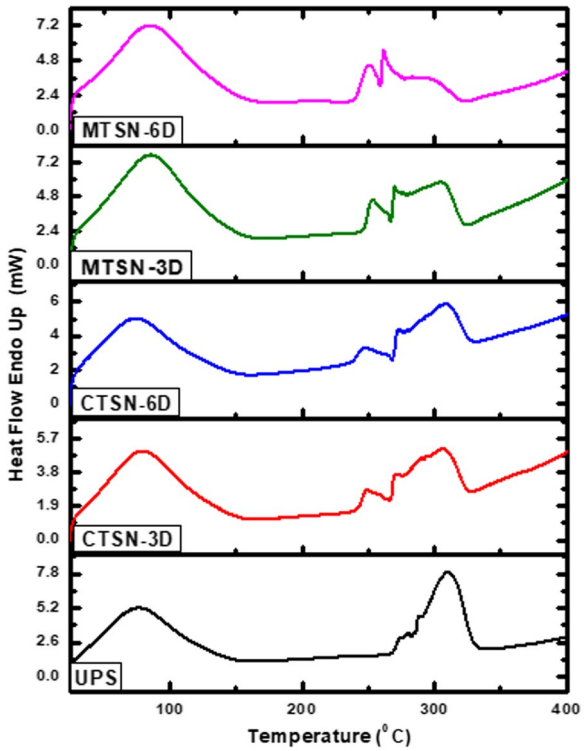

Fig. 2 The DSC thermograms for UPS, CTSN-3 days, CTSN-6 days, MTSN-3 days, and MTSN-6 days obtained during heating ranging from 25 to 400 °C at a heating speed of 10 °C/min. The evaluation of the differential scanning calorimetry (DSC) thermogram of untreated potato starch (UPS) versus chemically treated starch nanoparticle (CTSN) and mechanically treated starch nanoparticle (MTSN)

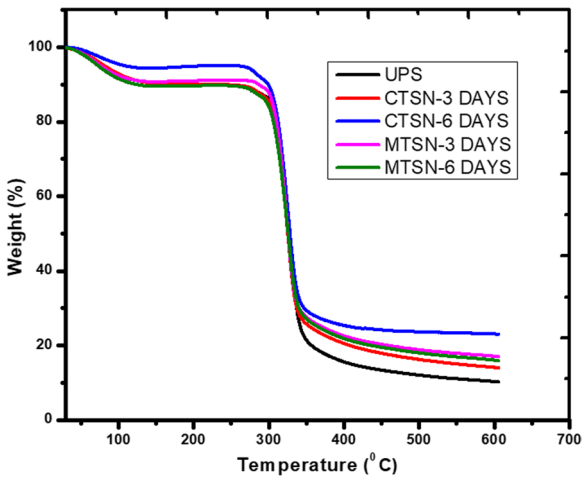

Fig. 3 The overlay of TGA curves obtained for UPS, CTSN-3 days, CTSN-6 days, MTSN-3 days, and MTSN-6 days during heating at a rate of 10 °C/min from 30 to 600 °C. The comparison of thermogravimetric analysis (TGA) curve of untreated potato starch (UPS) against chemically treated starch nanoparticle (CTSN) and mechanically treated starch nanoparticle (MTSN)

hydrogen bonding in a regulated pattern. The mechanical modification includes altering the characteristics of starch in a regulated manner using heat, friction from shaking, and moisture. The change alters the features of starch granules such as roughness, amylose content, and swelling strength. In addition, it encompasses the solubility index and the amount of water absorption capability [12, 28, 29].

Modification can be accomplished chemically by inserting a functional group into the starch molecule. This aids in bringing out the many changes in the starch molecule's varied features. Granular modifications of native starches can occur in chemical modifications, such as acid modification of starch, by treating the starch below its gelatinization temperature in an aqueous acid mixture, hydrolysis reduces the size of the granule as well as paste viscosity. Native starch is a semicrystalline polymer with different degrees of crystallinity because it is structured in alternating amorphous and crystalline lamellae in the granules. The amylopectin component of starch is solely responsible for crystallinity, whereas amylose is primarily responsible for amorphous areas [14, 28]. Amylose quantity reduced somewhat after acid alteration, while starch kept its native crystallinity pattern. The acid mostly affected the starch granule's amorphous areas [12, 30]. When a native starch is exposed to acid hydrolysis, the starch granules normally dissolve at the amylose area, while the amylopectin sections remain unchanged [31]. In conclusion, the development of SNP and SNC results in a decrease in amylose concentration because hydrolysis of starch by acid or enzymes causes a random decrease in chain length [12].

Morphology and particle size of starch nanoparticles

The top-down procedure was applied in both the chemical and mechanical methods of preparing starch nanoparticles in this study, in which nanoparticles were formed from structural and size refinement through a breakdown of bigger particles. The morphology and particle size of the starch nanoparticles generated were determined using SEM. CTSN and MTSN had diameters smaller than 1000 nm when compared to native or untreated starch, demonstrating the formation of sweet potato starch nanoparticles.

Scanning electron micrographs (Fig. 1) revealed that the particle appearance of MTSN was unaffected. The shape of the MTSN starch nanoparticles changed from spherical to irregular. In the literature, starch nanoparticles are often round, uneven, and rodlike in shape [32]. The incubation of the native starch in moisture with constant shaking and heating at 40 °C resulted in the diminution of the particle size of the starch granules due to mechanical friction from continuous shaking breaking

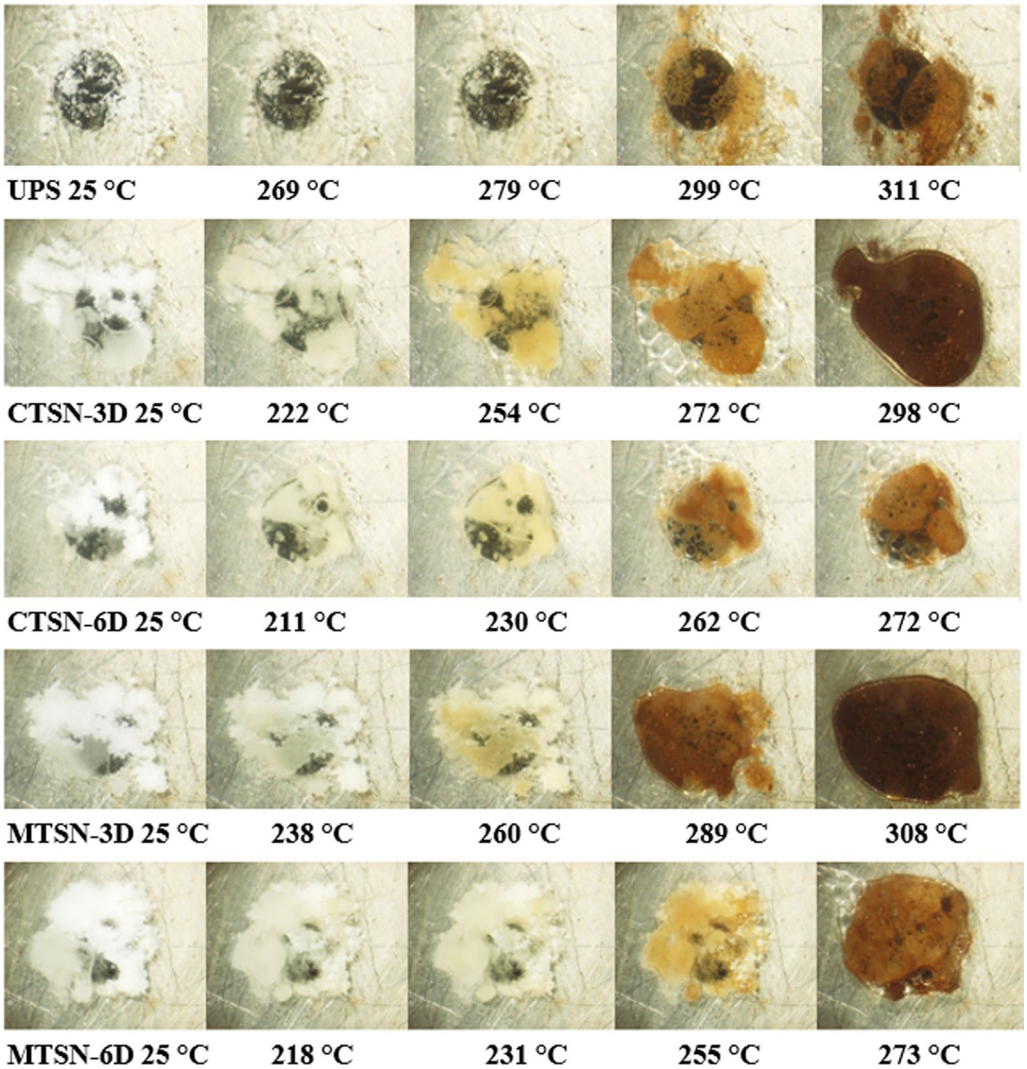

Fig. 4 Photomicrographs illustrating the thermal behavior of UPS, CTSN-3 days, CTSN-6 days, MTSN-3 days, and MTSN-6 days during heating at a rate of 10 °C/min. The overlay and comparison of hot-stage microscopy pictograms of untreated potato starch (UPS) versus chemically treated starch nanoparticles (CTSN) and mechanically treated starch nanoparticles (MTSN)

the covalent bonds of the starch particles. For processing times of 3 and 6 days, the size of native starch declined from the micro-range to the nano-range, resulting in starch nanoparticles (Table 1). The granular size of the MTSN processed in 3 days (683.35 nm ± 29.45) was smaller than the granular size of the MTSN processed in 6 days (729.03 nm ± 47.05).

SEM revealed that the untreated starch granules had some mild aggregation, but the treatment methods caused additional granule aggregation (Fig. 1). The effect of surface charge and particle size is the primary cause of nanoparticle aggregation. This is because there is a larger concentration of starch suspension present [11]. As a result of the strong acidic state and application heat at 40 °C, acid hydrolysis with hydrochloric acid caused severe disruption and rupture of the granular structure of the starch. The particle appearance of CTSN was significantly disrupted, which increased with processing time as spherical particles were transformed into irregular forms. CTSNs were nanoparticulate in size and smaller than untreated starch (Table 1). CTSN processed in 3 days (558.57 nm ± 38.33) had a smaller granular size than CTSN processed in 6 days (705.07 nm ± 23.89). Despite the fact that, in theory, longer treatment times during acid hydrolysis should be linked with greater size diminution because starch fragments are consecutively liberated from the granule surface, resulting in small particle size [11]. In summary, the particle

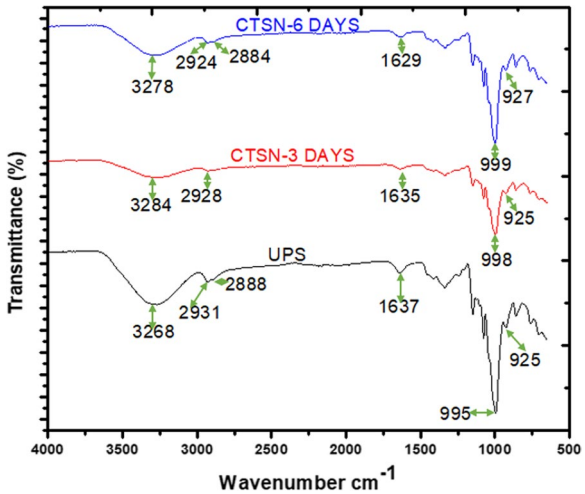

Fig. 5 The overlay of FTIR spectra of UPS, CTSN-3 days, and CTSN-6 days. The comparison of the Fourier transform infrared spectrum of untreated potato starch (UPS) against chemically treated starch nanoparticles (CTSN)

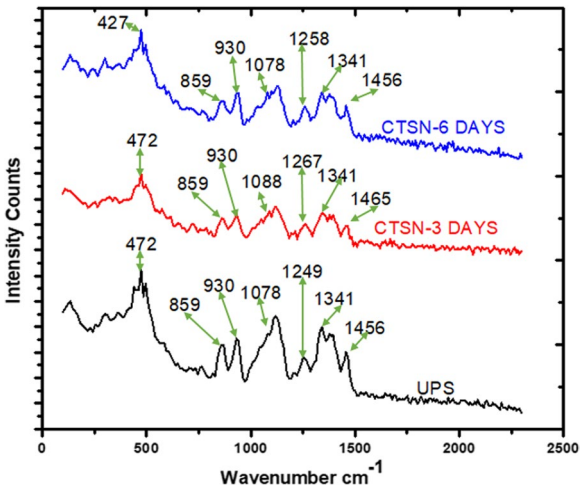

Fig. 7 The Raman spectra overlay of untreated starch and chemically treated starches. The comparison of the Raman spectrum of untreated potato starch (UPS) against chemically treated starch nanoparticles (CTSN)

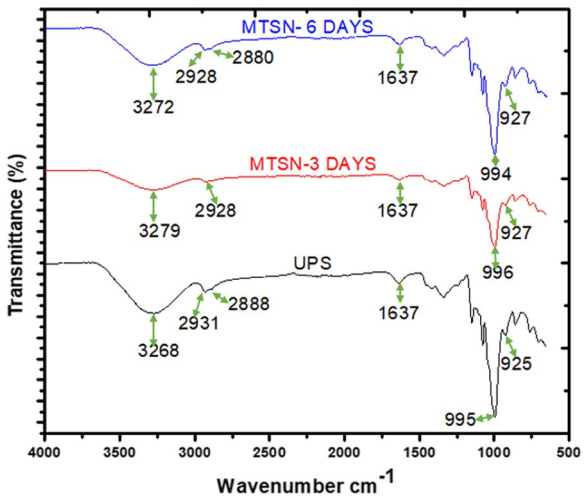

Fig. 6 The overlay of FTIR spectra of UPS, MTSN-3 days, and MTSN-6 days. The comparison of the Fourier transform infrared spectrum of untreated potato starch (UPS) against mechanically treated starch nanoparticles (MTSN)

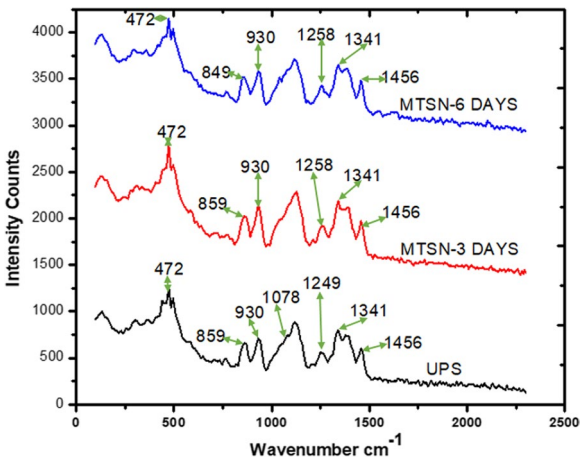

Fig. 8 The Raman spectra overlay of untreated starch and mechanically treated starches. The comparison of the Raman spectrum of untreated potato starch (UPS) versus mechanically treated starch nanoparticles (MTSN)

size of untreated potato starch was greater than that of treated starch in the following order: Untreated potato starch > MTSN-6 > MTSN-3 > CTSN-6 > CTSN-3.

Water absorption capacity (WAC) and solubility of treated and untreated starch

The WAC and solubility of starches are two essential functional characteristics. The treated starches had considerably greater ($p < 0.05$) WAC, which rose as processing time increased, except for CTSN-3 days (Table 2). The WAC of the treated starches and untreated starch were measured in the following order: CTSN-3 days > CTSN-6 days > MTSN-6 days > MTSN-3 days > untreated starch. WAC is determined by the starch sample's ability to hold water. The large increase in water absorption capacity of CTSN-3 days (94.45 ± 8.22), including other starch nanoparticles, compared to untreated starch (68.09 ± 1.02) can be attributed to a diminution in particle size, that resulted in a rise in surface area of starch nanoparticles formed. The mechanical and chemical hydrolysis of intermolecular connections inside starch granules allowed the hydrogen bonding sites in the granular structure to engage additional water in starch nanoparticles. Ahmad

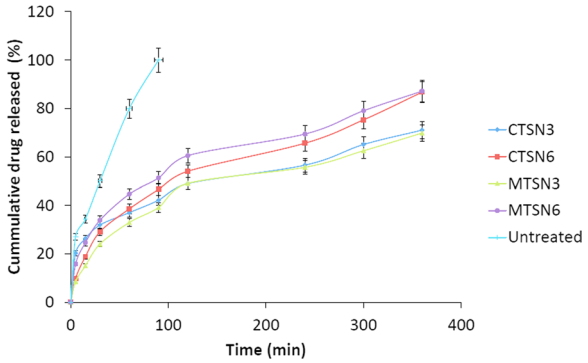

Fig. 9 Release profiles of ciprofloxacin-loaded chemically treated starch nanoparticles, mechanically treated starch nanoparticles, and untreated potato starch. The release study was conducted over a duration of 400 min

Table 1 Properties of ciprofloxacin-loaded untreated and treated potato starch

Code	Processing time	Particle size (nm)	Drug content (%)	Loading efficiency (%)
CTSN	3	558.57 ± 38.33	80.73	97.86
CTSN	6	605.07 ± 23.89	76.70	97.73
MTSN	3	683.35 ± 29.45	75.60	97.64
MTSN	6	729.03 ± 47.05	76.40	97.59
Untreated starch	0	15,600.87 ± 159.33	49.87	54.32

NB: CTSN, Chemically treated starch nanoparticles; MTSN, Mechanically treated starch nanoparticles

Table 2 Water absorption capacity and solubility of untreated and treated starch (mean ± SD; $n = 3$)

Code	Processing time	Water absorption capacity (%)	Solubility (%)
CTSN	3	94.45 ± 8.22	29.54 ± 3.48
CTSN	6	84.87 ± 9.38	34.09 ± 5.21
MTSN	3	72.32 ± 6.04	18.04 ± 3.34
MTSN	6	76.55 ± 4.83	22.45 ± 5.03
Untreated starch	0	68.09 ± 1.02	17.03 ± 0.36

NB: CTSN, Chemically treated starch nanoparticles; MTSN, Mechanically treated starch nanoparticles

et al. [33] found a similar finding for the WAC of starch nanoparticles made from underused and inexpensive polymer sources in a previous work.

The modified starches were more soluble than their native form ($p < 0.05$) (Table 2). However, CTSN-6 days (34.09 ± 5.21) demonstrated more solubility than MTSN-6 days (22.45 ± 5.03). The solubility of the treated and native starches increased in the following order: CTSN-6 days > CTSN-3 days > MTSN-6 days > MTSN -3 days > untreated starch. The increased solubility of CTSN-6 days compared to the other untreated starches may be attributed to the longer period for the hydrolysis of the starch granule, i.e., the starch was exposed to acid treatment for a longer period of time. Because of their broken starch granule, treated or modified starches are soluble in cold water, whereas native or untreated starches have limited water solubility. Native starch can only absorb water in a reversible manner [34]. As previously stated, when a native starch is mechanically or chemically modified, the amorphous area or pattern is disrupted, resulting in a decline in amylose content and a rise in amylopectin content, which enhances the crystallinity of the modified starch. The enhanced WAC and solubility power of treated starches are attributed to the increased amylopectin content and higher concentration of phosphorus groups. The presence of these phosphorus groups on neighboring chains promotes repulsion, resulting in increased hydration due to the weakening of the strong connections inside the amylopectin or crystalline area [35].

Thermal analysis of the untreated and treated starches

Thermal analysis methods including hot-stage microscopy (HSM), differential scanning calorimetry (DSC), and thermogravimetric analysis (TGA) were utilized to test the temperature stability (such as isothermal, cooling, or heating) of the UPS and treated starches. These procedures were employed to analyze the physiochemical characteristics of excipients namely melting, evaporation, sublimation, dehydration, phase transitions, oxidation, degradation, and decomposition [36–39]. HSM was utilized to supplement the results of DSC and TGA.

Differential scanning calorimetry (DSC)

DSC can be employed to determine the transition temperatures of onset [T_o], midpoint [T_p], conclusion [T_c], and gelatinization enthalpy. These gelatinization characteristics can be used to identify a sample's crystallinity or amorphousness [35].

Figure 2 displays the endotherms and exotherms for untreated and treated potato starches (chemically and mechanically treated starches). The DSC properties of various starches are listed in Table 3. The endothermic peaks observed by all of the starches thermograms at lower temperatures were caused by starch gelatinization [40]. The gelatinization temperatures (T_o and T_p) increased with chemical (CTSN-3 days-42.23 °C, 79.29 °C) and mechanical (MTSN-3 days-43.89 °C, 85.68 °C and MTSN-6 days-43.06 °C, 85.01 °C) treatments of the native starch (40.40 °C, 76.21 °C) except for

Table 3 Differential scanning calorimetry (DSC) characteristics of untreated potato starch (UPS), chemically treated starch nanoparticle (CTSN), and mechanically treated starch nanoparticle (MTSN)

Sweet potato starches	Endothermic peak (1)		Endothermic peak (2)		Exothermic peak
	T_o (°C)	T_p (°C)	T_o (°C)	T_p (°C)	T_p (°C)
UPS	40.40	76.21	263.92	309.80	336.44
CTSN-3 days	42.23	79.29	227.28	306.49	330.68
CTSN-6 days	39.77	74.16	230.58	308.97	329.85
MTSN-3 days	43.89	85.68	238.91	305.68	324.80
MTSN-6 days	43.06	85.01	228.94	262.28	322.33

Gelatinization temperature parameters (in °C) = onset temperature (T_o), peak temperature (T_p)

Table 4 Thermogravimetric analysis (TGA) thermal events obtained for untreated potato starch (UPS), chemically treated starch nanoparticles (CTSN), and mechanically treated starch nanoparticle

Sweet potato starches	T_o (°C)	T_{max} (°C)	% Mass loss by degradation
UPS	279.60	362.35	69.03
CTSN-3 days	274.19	354.12	64.14
CTSN-6 days	263.37	352.77	65.96
MTSN-3 days	260.67	358.15	64.78
MTSN-6 days	257.97	356.82	63.50

T_o, onset of degradation temperature; T_{max}, maximum temperature of degradation

CTSN-6 days (39.77 °C, 74.16 °C). According to the DSC results, MTSN-3 days had the greatest gelatinization temperatures, whereas CTSN-6 days had the lowest.

The rise in T_p of gelatinization of CTSN-3 days after acidic treatment of *Ipomoea batatas* starch indicates that a considerable amount of the amorphous area of this starch granule was hydrolyzed and changed to crystalline structure or pattern. This finding is consistent with earlier research works [30, 41]. There was a considerable increase in T_p of gelatinization of MTSN-3 days and MTSN-6 days after mechanically modifying sweet potato starch. Mechanical treatment of native sweet potato employing heat, moisture, and shaking for 3 and 6 days reduced amylose concentration, resulting in increased crystallinity of the modified starch granule. Thus, mechanical modification of native starch for 3 days was more successful than 6 days in producing starch nanoparticles. According to the literature, the affiliations of amylose chains within the amorphous area and/or the order of crystallinity in sweet potato starch were altered following heat–moisture–treatment [41, 42].

Endothermic peaks were seen at 220–310 °C before the exothermic peaks in all of the starches. The endothermic peaks were created by the breakdown of long chains in the various starches granules during heating in the DSC. High amylopectin content requires elevated temperature for long-chain breakdown [43]. The temperatures required to break down the long chains in the sample are calculated in Table 3, and they were 45.88 °C, 79.21 °C, 78.39 °C, 66.77 °C, and 33.34 °C for UPS, CTSN-3 days, CTSN-6 days, MTSN-3 days, and MTSN-6 days, respectively. As a result, chemically treated starch nanoparticles had the most amylopectin and would require more energy to break down their lengthy chains. In summary, when compared to the other modified polymers, chemically treated starch nanoparticles processed for 3 days produced the most crystalline nano-carrier.

Exothermic peaks above 320 °C were seen in all samples, indicating starch breakdown. These results corresponded to the maximum temperature of deterioration obtained in thermogravimetric analysis (TGA) curves for all samples. DSC thermograms typically exhibit an exothermic peak due to energy release from the oxidation of the studied sample [43].

Thermogravimetric analysis (TGA)

TGA can be utilized to calculate the sample's percentage mass loss as a result of temperature increase over time. Based on the sample's commencement of degradation temperature, this technique can be used to estimate its thermal stability and decomposition. In addition, it detects moisture and volatile solvents in samples [44–46]. TGA curves and thermal events of untreated potato starch and treated potato starches (chemically and mechanically treated starches) processed for 3 and 6 days are shown in Fig. 3 and Table 4. All of the TGA curves demonstrated three significant mass loss portions. For untreated and treated potato starches, the first stage of mass loss begins as soon as the temperature rises (73.75 °C) and finishes at roughly 142.83 °C. This showed that residual solvents were present in all of the samples. At this point, the percentage mass loss is determined by the moisture content of both the treated and untreated potato starches.

The TGA curves of UPS, CTSN-3 days, CTSN-6 days, MTSN-3 days, and MTSN-6 days (Fig. 3) showed thermal stability until 279.60 °C, 274.19 °C, 263.37 °C, 260.67 °C, and 257.97 °C, respectively. Thus, the order of stability of the native and modified starches was UPS > CTSN-3 days > CTSN-6 days > MTSN-3 days > MTSN-6 days.

The second stage of mass loss is the starch's principal degradation process, which finished at about 370 °C (Table 4). Previous research utilizing TGA revealed that the maximal degradation temperature of native sweet potato starch was 350 °C [40]. This study's findings are supported by the mentioned literature. UPS had the maximum mass loss through degradation at a speed of 10 °C/min over a temperature limit of 279.60–362.35 °C, whereas MTSN-6 days had the lowest mass loss at 63.50% from 257.97 to 356.82 °C. The percentage mass loss by degradation of untreated starch relative to treated starch was in the following order: MTSN-6 days < CTSN-3 days < MTSN-3 days < CTSN-6 days < UPS.

Hot-stage microscopy (HSM)

HSM enables the visual monitoring of changes in a sample's physicochemical characteristics or thermal behavior caused by heating. The thermal behaviors of the samples during TGA and DSC analysis were corroborated by the HSM micrograph in Fig. 4. During the HSM examination of the untreated and treated starches, UPS was shown to be the most stable to heating when compared to the treated starches. UPS > MTSN-3 days > CTSN-3 days > MTSN-6 days > CTSN-6 days was the order of stability. UPS degradation temperature peak on HSM (279 °C) coincided with TGA degradation onset (279.60 °C). The yellowish-brown staining shown in the photomicrographs suggests that the samples were carbonized at temperatures exceeding 260 °C. The ensuing dark-brown hue at the end of the analyses indicated the breakdown of the starches' long chains and small rings [40, 42].

FTIR analysis

FTIR is employed to ascertain the existence of functional groups in a given sample [47]. Figures 5 and 6 displayed the FTIR spectra of untreated and treated potato starches. The FTIR absorption bands of untreated potato starch were compared to those of starch nanoparticles generated using chemical and mechanical methods at two different processing times (Tables 5 and 6). The hydroxyl group, which is a typical peak of native starch, corresponds to the strong broad absorbance band observed at 3268 cm^{-1} for untreated potato starch (UPS) [48]. The vibration stretching of the methyl and methylene C–H bonds causes the doublet peaks at 2931 cm^{-1} and 2888 cm^{-1}, respectively [34]. Closely linked water molecules, C–O stretching vibration, and glycosidic linkage (C–O–C) were ascribed to the IR absorption bands

Table 5 Table of untreated potato starch (UPS) and chemically treated starch nanoparticles (CTSN) wavenumbers depicted in FTIR analysis with corresponding functional groups

UPS		CTSN-3 days		CTSN-6 days		Functional group
Wavenumber (cm^{-1})	Description	Wavenumber (cm^{-1})	Description	Wavenumber (cm^{-1})	Description	
3268	Strong broad peak	3284	Weak broad peak	3278	Medium broad peak	O–H
2931	Weak peak	2928	Weak peak	2924	Weak peak	C–H
2888	Very weak peak	–	–	2884	Very weak peak	C–H
1637	Weak broad peak	1635	Very weak broad peak	1629	Weak broad peak	H_2O
995	Strong sharp peak	998	Medium sharp peak	999	Strong sharp peak	C–O
925	Weak sharp peak	925	Weak sharp peak	927	Weak sharp peak	C–O–C

Table 6 Table of untreated potato starch (UPS) and mechanically treated starch nanoparticles (MTSN) wavenumbers depicted in FTIR analysis with corresponding functional groups

UPS		MTSN-3 days		MTSN-6 days		
Wavenumber (cm^{-1})	Description	Wavenumber (cm^{-1})	Description	Wavenumber (cm^{-1})	Description	Functional group
3268	Strong broad peak	3279	Weak broad peak	3272	Strong broad peak	O–H
2931	Weak peak	2928	Weak peak	2928	Weak peak	C–H
2888	Very weak peak	–	–	2880	Very weak peak	C–H
1637	Weak broad peak	1637	Very weak broad peak	1637	Weak broad peak	H_2O
995	Strong sharp peak	996	Medium sharp peak	994	Strong sharp peak	C–O
925	Weak sharp peak	927	Very weak sharp peak	927	Weak sharp peak	C–O–C

at 1637 cm^{-1}, 995 cm^{-1}, and 925 cm^{-1}, respectively [34, 48, 49].

The FTIR spectra of CTSN (Fig. 5) showed reductions in the intensity of distinctive peaks of CTSN-3 days and CTSN-6 days, when compared to UPS. Comparing the native potato starch absorption bands with modified starches, there were small shifts in almost all of the CTSN generated distinctive peaks' IR absorption bands (Table 5), but they have similar functional groups. The vibration stretching of the methylene C–H bond, which was present in UPS (2888 cm^{-1}) was absent in CTSN-3 days, but was present in CTSN-6 days with a somewhat lower band (2884 cm^{-1}).

When compared to UPS, the FTIR spectra of MTSN (Fig. 6) showed declines in the intensity of distinctive peaks of MTSN-3 and MTSN-6 days. Compared to the native potato starch absorption bands, there were minor shifts in almost all of the characteristic peaks of the MTSN generated (Table 6), but all of the characteristic functional groups from the untreated starch were intact. The vibration stretching of the methylene C–H bond, which was seen in UPS (2888 cm^{-1}), was absent in MTSN-3 days but present in MTSN-6 days with a lower band (2880 cm^{-1}).

The reduction in the intensity of characteristic peaks at C–H stretching can be ascribed to changes in the level of amylose and amylopectin content existing in the modified starches [49, 50] The results showed that both acidic and mechanical treatment time on native starch had effects on the amylose and amylopectin content present in starch. Minor changes in the absorption bands of the peak or slight shift in position of the peak between the ranges of 2970 cm^{-1} to 2910 cm^{-1} signified the stretching vibration of C–C–H bond [51]. *Ipomoea batatas* starch usually have high amylopectin content and crystallinity [52]. The slight shift of the absorption band 2931 cm^{-1} to lower bands at 2928 cm^{-1} and 2924 cm^{-1} CTSN 3 days and CTSN 6 days respectively and also for MTSN 3 days and MTSN 6 days at 2928 cm^{-1}, signifies the increase in amylopectin content, thus leading to increase in the crystallinity of the modified starches. From a previous study, observable reduction in the peak intensity at 1635 cm^{-1} and 1637 cm^{-1} for CTSN 3 days and MTSN 3 days respectively (Tables 5 and 6) compared to USP (1637 cm^{-1}) means that as the crystallinity of two chemically and mechanically treated starch for 3 days increases, the absorption bands become weaker [52].

The decrease in the intensity of distinctive peaks during C–H stretching can be attributed to changes in the amylose and amylopectin content of the modified starches [49, 50]. The results demonstrated that the amylose and amylopectin concentration of native starch was affected by both acidic and mechanical treatment duration. Minor variations in the peak's absorption bands or a slight shift in peak position between 2970 and 2910 cm^{-1} indicated the stretching vibration of the C–C–H bond [51]. Sweet potato starch is often high in amylopectin and crystallinity [52]. The slight shift of the absorption band 2931 cm^{-1} to lower bands at 2928 cm^{-1} and 2924 cm^{-1} for CTSN-3 days and CTSN-6 days, respectively, as well as for MTSN-3 days and MTSN-6 days at 2928 cm^{-1}, indicates a rise in amylopectin content, which leads to intensification in crystallinity of the modified starches. According to a previous study, the observable decrease in peak intensity at 1635 cm^{-1} and 1637 cm^{-1} for CTSN-3 days and MTSN-3 days, respectively (Tables 5 and 6) compared to USP (1637 cm^{-1}) means that as the crystallinity of two chemically and mechanically treated starches increases for 3 days, the absorption bands become weaker [52].

RAMAN characterization

The structural fingerprints obtained by Raman spectroscopy can be used to identify samples [52, 53]. Raman is typically used to supplement FTIR data [38]. In some circumstances, Raman will detect vibration patterns that FTIR would not detect, and vice versa [54, 55]. Figures 7 and 8 show the Raman spectra of untreated and treated potato starches. Tables 7 and 8 display the similarities and differences in the characteristic bands of UPS and the treated starches. The UPS spectra revealed prominent peaks at 472 cm^{-1}, 859 cm^{-1}, 930 cm^{-1}, 1078 cm^{-1}, 1249 cm^{-1}, 1341 cm^{-1}, and 1456 cm^{-1}, which aided in the identification of the untreated starch. Skeletal modes, CH and CH2 deformation, bending vibration of C–O–H, and C–O–H bending were given to characteristic bands at 472 cm^{-1}, 859 cm^{-1}, 930 cm^{-1}, and 1078 cm^{-1}, respectively. Furthermore, significant absorption bands at 1249 cm^{-1}, 1341 cm^{-1}, and 1456 cm^{-1} were associated with the CH_2 OH-related mode functional group, vibration CH_2 twisting and bending of C–O–H, and CH_2 deformation, respectively. These characteristic peaks are similar to those described in the literature [50]. The CTSN spectra (Fig. 7) demonstrated that it kept almost all of the UPS peaks with just negligible changes in peak strength. MTSN spectra (Fig. 8) revealed that UPS major peaks were kept with nearly the same intensity count, but the distinctive peak at 1078 cm^{-1} was missing in both MTSN-3 and MTSN-6 days.

In vitro release profile of the ciprofloxacin-loaded starch nanoparticles

In comparison with the untreated starch (Fig. 9 and Table 9), release times were significantly longer for the chemically and mechanically modified starches in the rank order of t80, CTSN-3 > MTSN-3 > > CTSN-6 > MT

Table 7 Untreated potato starch (UPS) wavenumbers portrayed in Raman analysis with corresponding functional groups compared to chemically treated starch nanoparticles (CTSN-3 days and CTSN-6 days) absorption spectrum

UPS		CTSN-3 days		CTSN-6 days		
Wavenumber (cm^{-1})	Description	Wavenumber (cm^{-1})	Description	Wavenumber (cm^{-1})	Description	Functional group
472	Strong	472	Medium	472	Strong	Skeletal modes
859	Medium	859	Weak	859	Weak	CH and CH_2 (deformation)
930	Medium	930	Weak	930	Medium	C–O–H (bending)
1078	Strong	1088	Medium	1078	Medium	C–O–H (bending)
1249	Weak	1267	Weak	1258	Weak	CH_2 OH
1341	Strong	1341	Medium	1341	Medium	CH_2 (twist) C–O–H (bending)
1456	Medium	1465	Weak	1456	Medium	CH_2 (deformation)

Table 8 Untreated potato starch (UPS) wavenumbers portrayed in Raman analysis with corresponding functional groups compared to mechanically treated starch nanoparticles (MTSN-3 days and MTSN-6 days) absorption spectrum

UPS		MTSN-3 days		MTSN-6 days		
Wavenumber (cm^{-1})	Description	Wavenumber (cm^{-1})	Description	Wavenumber (cm^{-1})	Description	Functional group
472	Strong	472	Strong	472	Strong	Skeletal modes
859	Medium	859	Medium	849	Medium	CH and CH_2 (deformation)
930	Medium	930	Medium	930	Medium	C–O–H (bending)
1078	Strong	–	–	–	–	C–O–H (bending)
1249	Weak	1258	Weak	1258	Weak	CH_2 OH
1341	Strong	1341	Strong	1341	Strong	CH_2 (twist) C–O–H (bending)
1456	Medium	1456	Medium	1456	Medium	CH_2 (deformation)

Table 9 Release times of ciprofloxacin-loaded untreated potato starch and starch nanoparticles

Formulation code	Dissolution times			
	T_{25} (min)	T_{50} (min)	T_{80} (min)	T_{90} (min)
CTSN-3 days	14.46	133.96	606.15 (10.1 h)	884.87
CTSN-6 days	23.76	112.89	324.84	423.34
MTSN-3 days	33.16	167.69	503.22	662.76
MTSN-6 days	13.50	85.95	301.54	413.00
Untreated starch	7.33	25.97	61.27 (1.0 h)	75.97

NB, CTSN, Chemically treated starch nanoparticles; MTSN, Mechanically treated starch nanoparticles

SN-6 > > > untreated starch. The untreated starch demonstrated immediate release, where 80% of drug was achieved in 61 min.

All the nanoformulations, irrespective of method and processing times, and the untreated starch demonstrated release properties which fitted the Korsmeyer–Peppas model ($Qt/Qa = kkt^n$) (Table 10). The model is typically known as "Power law," and it describes the drug dissolution from a polymeric system such as starch used in this study. The kinetics of drug release was indicated by the constant n in Korsmeyer–Peppas model ($Qt/Qa = kkt^n$). The constant n is the diffusional exponent or release exponent, indicative of the drug release mechanism. All the nanoformulations demonstrated $n < 0.5$, while the untreated starch had $n > 0.5 < 1.0$. When $0.5 < n < 1.0$, it indicates anomalous (non-Fickian) diffusion. The nanoformulations and the untreated starch thus had release which followed non-Fickian diffusion [56].

Conclusion

The characteristics of the produced starch nanoparticles were regulated by techniques and processing time. Particle sizes rose as processing time increased, which was not a good thing. Chemically created starch nanoparticles had longer release times than mechanically prepared starch nanoparticles, and shorter processing times appeared to be more favorable in both preparation processes. Chemically treated starch nanoparticles for 3 days demonstrated the smallest particle

Table 10 Correlation coefficients (R^2) obtained for ciprofloxacin-loaded nanoparticles

Code	Zero order R^2	First order	Higuchi	Hixson–Crowell	Korsmeyer–Peppas	*n*
CTSN-3	0.2595	0.6081	0.8820	0.5061	0.9915	0.311
CTSN-6	0.6816	0.9187	0.9869	0.8653	0.9929	0.445
MTSN-3	0.6320	0.8528	0.9775	0.7909	0.9885	0.428
MTSN-6	0.4935	0.8678	0.9548	0.7879	0.9945	0.374
Untreated starch	0.8480	0.9535	0.9864	0.9525	0.9891	0.548

sizes, maximum drug content, loading efficiency, and percentage water absorption capacity; it can thus be enhanced as a ciprofloxacin carrier. These findings demonstrated that varied processing methods and time can alter the features of nanoparticles created from a specific polymer, and they will aid in the development of recommendations for developing future nanoparticles.

Abbreviations

CTSN	Chemically treated starch nanoparticles
UPS	Untreated potato starch
MTSN	Mechanically treated starch nanoparticles
$T_{80\%}$	Time of 80% of drug release
SNPs	Starch nanoparticles
WAC	Water absorption capacity
W	Weight
x	Weight of drug in starch nanoparticle
y	Weight of starch nanoparticle
a	Weight of drug in starch nanoparticle
b	First weight of drug in loading solution
SEM	Scanning electron microscopy
DSC	Differential scanning calorimetry
TGA	Thermogravimetric analysis
HSM	Hot-stage microscopy
FTIR	Fourier transform infrared spectroscopy
SNCs	Starch nanocrystals
T_o	Onset gelatinization temperature
T_p	Peak gelatinization temperature
T_o	Onset of degradation temperature
T_{max}	Maximum temperature of degradation
T	Time of drug release
min	Minutes
R^2	Correlation coefficients
n	Release exponent

Acknowledgements
Not applicable.

Author contributions
TOA (Tolulope Omolola Ajala) designed the research concept, extraction of starch, supervision of laboratory work, revision of drafts of manuscript, and approval of the final manuscript. OAO (Omobolanle Ayoyinka Omoteso) conducted some of the experiments, interpreted the results and wrote part of the manuscript relating to such experiments, revised the manuscript, and formatted the manuscript to journal specification, and OMA (Oladotun Micheal Awe) conducted some of the experiments, wrote first draft of the manuscript, and participated in approving the final manuscript. All authors read and approved the final manuscript.

Funding
This study got no funding from any organization or individual.

Availability of data and materials
The data that support the findings of this study are available from the corresponding author, upon reasonable request.

Declarations

Ethics approval and consent to participate
This study did not include any human or animal subjects.

Consent for publication
The authors declare no conflict of interest.

Competing interests
The authors declare that they have no competing interests.

Received: 19 February 2023 Accepted: 18 April 2023
Published online: 28 April 2023

References
1. Biswas AK, Islam MR, Choudhury ZS, Mostafa A, Kadir MF (2014) Nanotechnology based approaches in cancer therapeutics. Adv Nat Sci Nanosci Nanotechnol 5(4):043001. https://doi.org/10.1088/2043-6262/5/4/043001
2. Farokhzad OC, Langer R (2009) Impact of nanotechnology on drug delivery. ACS Nano 3(1):16–20. https://doi.org/10.1021/nn900002m
3. Levins CG, Schafmeister CE (2005) The synthesis of curved and linear structures from a minimal set of monomers. J Org Chem 70(22):9002–9008. https://doi.org/10.1021/jo051639u
4. Odeniyi MA, Omoteso OA, Adepoju AO, Jaiyeoba KT (2018) Starch nanoparticles in drug delivery: a review. Polim W Med 48:41–45. https://doi.org/10.17219/pim/99993
5. Zhang J, Saltzman M (2013) Engineering biodegradable nanoparticles for drug and gene delivery. Chem Eng Progress 109(3):25
6. Le Corre D, Bras J, Dufresne A (2010) Starch nanoparticles: a review. Biomacromol 11(5):1139–1153. https://doi.org/10.1021/bm901428y
7. Smith AM (2001) The biosynthesis of starch granules. Biomacromol 2(2):335–341. https://doi.org/10.1021/bm000133c
8. Santana ÁL, Meireles MAA (2014) New starches are the trend for industry applications: a review. Food public health 4(5):229–241. https://doi.org/10.5923/j.fph.20140405.04
9. Torres FG, Arroyo J, Tineo C, Troncoso O (2019) Tailoring the properties of native andean potato starch nanoparticles using acid and alkaline treatments. Starch 71(3–4):1800234. https://doi.org/10.1002/star.201800234
10. Campelo PH, Sant'Ana AS, Clerici MTPS (2020) Starch nanoparticles: production methods, structure, and properties for food applications. Curr Opin Food Sci 33:136–140. https://doi.org/10.1016/j.cofs.2020.04.007
11. Chavan P, Sinhmar A, Nehra M, Thory R, Pathera AK, Sundarraj AA, Nain V (2021) Impact on various properties of native starch after synthesis of

starch nanoparticles: a review. Food Chem 364:130416. https://doi.org/10.1016/j.foodchem.2021.130416
12. LeCorre D, Bras J, Dufresne A (2011) Influence of botanic origin and amylose content on the morphology of starch nanocrystals. J Nanopart Res 13(12):7193–7208. https://doi.org/10.1007/s11051-011-0634-2
13. Odeniyi MA, Adepoju AO, Jaiyeoba KT (2019) Native and modified Digitaria exilis starch nanoparticles as a carrier system for the controlled release of naproxen. Starch 71(9–10):1900067. https://doi.org/10.1002/star.201900067
14. Gallant DJ, Bouchet B, Baldwin PM (1997) Microscopy of starch: evidence of a new level of granule organization. Carbohydr Polym 32(3–4):177–191. https://doi.org/10.1016/S0144-8617(97)00008-8
15. Tang H, Mitsunaga T, Kawamura Y (2006) Molecular arrangement in blocklets and starch granule architecture. Carbohydr Polym 63(4):555–560. https://doi.org/10.1016/j.carbpol.2005.10.016
16. Kim HY, Park SS, Lim ST (2015) Preparation, characterization and utilization of starch nanoparticles. Colloids Surf B 126:607–620. https://doi.org/10.1016/j.colsurfb.2014.11.011
17. Alam MK (2021) A comprehensive review of sweet potato (*Ipomoea batatas* [L.] Lam): revisiting the associated health benefits. Trends Food Sci Technol 115:512–529. https://doi.org/10.1016/j.tifs.2021.07.001
18. Ugoeze KC, Idris ME (2020) Development of co-processed powders containing lactose, *Mucuna flagellipes* seed gum and Ipomoea batatas tuber starch. Int J Appl Bio Pharma Technol 11(4):256–275
19. Odeku OA (2013) Potentials of tropical starches as pharmaceutical excipients: a review. Starch 65(1–2):89–106. https://doi.org/10.1002/star.201200076
20. Charoo NA, Kohli K, Ali A, Anwer A (2003) Ophthalmic delivery of ciprofloxacin hydrochloride from different polymer formulations: in vitro and in vivo studies. Drug Dev Ind Pharm 29(2):215–221. https://doi.org/10.1081/DDC-120016729
21. Gutiérrez-Castrellón P, Díaz-García L, de Colsa-Ranero A, Cuevas-Alpuche J, Jiménez-Escobar I (2015) Efficacy and safety of ciprofloxacin treatment in urinary tract infections (UTIs) in adults: a systematic review with meta-analysis. Gac Med Mex 151:225–244
22. Tehler U, Fagerberg JH, Svensson R, Larhed M, Artursson P, Bergström CA (2013) Optimizing solubility and permeability of a biopharmaceutics classification system (BCS) class 4 antibiotic drug using lipophilic fragments disturbing the crystal lattice. J Med Chem 56(6):2690–2694. https://doi.org/10.1021/jm301721e
23. Ajala TO, Silva BO (2020) The design of ibuprofen-loaded microbeads using polymers obtained from *Xanthosoma sagittifolium* and *Dillenia indica*. Polym Med 50(1):21–31. https://doi.org/10.17219/pim/122015
24. Kim HY, Park DJ, Kim JY, Lim ST (2013) Preparation of crystalline starch nanoparticles using cold acid hydrolysis and ultrasonication. Carbohydr Polym 98(1):295–301. https://doi.org/10.1016/j.carbpol.2013.05.085
25. Akin-Ajani OD, Itiola OA, Odeku OA (2014) Effect of acid modification on the material and compaction properties of fonio and sweet potato starches. Starch 66(7–8):749–759
26. Ngilirabanga JB, Aucamp M, Samsodien H (2021) Mechanochemical synthesis and characterization of Zidovudine-lamivudine solid dispersion (binary eutectic mixture). J Drug Deliv Sci Technol 64:102639. https://doi.org/10.1016/j.jddst.2021.102639
27. Ajala TO, Abraham A, Keck CM, Odeku OA, Elufioye TO, Olopade JO (2021) Shea butter (*Vitellaria paradoxa*) and Pentaclethra macrophylla oil as lipids in the formulation of Nanostructured lipid carriers. Sci Afr 13:e00965. https://doi.org/10.1016/j.sciaf.2021.e00965
28. Kumari S, Yadav BS, Yadav RB (2020) Synthesis and modification approaches for starch nanoparticles for their emerging food industrial applications: a review. Food Res Int 128:108765. https://doi.org/10.1016/j.foodres.2019.108765
29. Goel C, Semwal AD, Khan A, Kumar S, Sharma GK (2020) Physical modification of starch: changes in glycemic index, starch fractions, physicochemical and functional properties of heat-moisture treated buckwheat starch. J Food Sci Technol 57(8):2941–2948. https://doi.org/10.1007/s13197-020-04326-4
30. Wang L, Wang YJ (2001) Structures and physicochemical properties of acid-thinned corn, potato and rice starches. Starch 53(11):570–576. https://doi.org/10.1002/1521-379X(200111)53:11%3C570::AID-STAR570%3E3.0.CO;2-S
31. Song S, Wang C, Pan Z, Wang X (2008) Preparation and characterization of amphiphilic starch nanocrystals. J Appl Polym Sci 107(1):418–422. https://doi.org/10.1002/app.27076
32. Sun Q (2018) Starch nanoparticles. In: Starch in food. Woodhead Publishing, pp 691–745. https://doi.org/10.1016/B978-0-08-100868-3.00018-4
33. Ahmad M, Gani A, Hassan I, Huang Q, Shabbir H (2020) Production and characterization of starch nanoparticles by mild alkali hydrolysis and ultra-sonication process. Sci Rep 10(1):1–11. https://doi.org/10.1038/s41598-020-60380-0
34. Fang JM, Fowler PA, Tomkinson J, Hill CS (2002) The preparation and characterization of a series of chemically modified potato starches. Carbohydr polym 47(3):245–252. https://doi.org/10.1016/S0144-8617(01)00187-4
35. Hoover R (2001) Composition, molecular structure, and physicochemical properties of tuber and root starches: a review. Carbohydr polym 45(3):253–267. https://doi.org/10.1016/S0144-8617(00)00260-5
36. Gaisford S, Kett V, Haines P (eds) (2019). Royal Society of Chemistry
37. Kumar A, Singh P, Nanda A (2020) Hot stage microscopy and its applications in pharmaceutical characterization. Appl Microsc 50(1):1–11. https://doi.org/10.1186/s42649-020-00032-9
38. Law D, Zhou D (2017) Solid-state characterization and techniques. In: Developing solid oral dosage forms. Academic Press, pp 59–84. https://doi.org/10.1016/B978-0-12-802447-8.00003-0
39. Patel P, Ahir K, Patel V, Manani L, Patel C (2015) Drug-Excipient compatibility studies: First step for dosage form development. Pharma Innov 4(5):14
40. Liu Y, Yang L, Ma C, Zhang Y (2019) Thermal behavior of sweet potato starch by non-isothermal thermogravimetric analysis. Materials 12(5):699. https://doi.org/10.3390/ma12050699
41. Singh S, Raina CS, Bawa AS, Saxena DC (2005) Effect of heat-moisture treatment and acid modification on rheological, textural, and differential scanning calorimetry characteristics of sweetpotato starch. J Food Sci 70(6):e373–e378. https://doi.org/10.1111/j.1365-2621.2005.tb11441.x
42. Hoover R, Vasanthan T (1994) Effect of heat-moisture treatment on the structure and physicochemical properties of cereal, legume, and tuber starches. Carbohydr Res 252:33–53. https://doi.org/10.1016/0008-6215(94)90004-3
43. Liu X, Yu L, Liu H, Chen L, Li L (2009) Thermal decomposition of corn starch with different amylose/amylopectin ratios in open and sealed systems. Cereal Chem 86(4):383–385. https://doi.org/10.1094/CCHEM-86-4-0383
44. Ebnesajjad S (2011) Surface and material characterization techniques. In: Handbook of adhesives and surface preparation. William Andrew Publishing, pp 31–48. https://doi.org/10.1016/B978-1-4377-4461-3.10004-5
45. Liu X, Wang Y, Yu L, Tong Z, Chen L, Liu H, Li X (2013) Thermal degradation and stability of starch under different processing conditions. Starch 65(1–2):48–60. https://doi.org/10.1002/star.201200198
46. Scrivens G, Ticehurst M, Swanson JT (2018) Strategies for improving the reliability of accelerated predictive stability (APS) studies. In: Accelerated predictive stability. Academic Press, pp 175–206. https://doi.org/10.1016/B978-0-12-802786-8.00007-3
47. Khan SA, Khan SB, Khan. U, Farooq A, Akhtar K, Asiri AM (2018) Fourier transform infrared spectroscopy: fundamentals and application in functional groups and nanomaterials characterization. In: Handbook of materials characterization. Springer, Cham, pp 317–344. https://doi.org/10.1007/978-3-319-92955-2_9
48. Wu J, Huang Y, Yao R, Deng S, Li F, Bian X (2019) Preparation and characterization of starch nanoparticles from potato starch by combined solid-state acid-catalyzed hydrolysis and nanoprecipitation. Starch 71(9–10):1900095. https://doi.org/10.1002/star.201900095
49. Babu AS, Parimalavalli R, Jagannadham K, Rao JS (2015) Chemical and structural properties of sweet potato starch treated with organic and inorganic acid. J Food Sci Tech 52(9):5745–5753. https://doi.org/10.1007/s13197-014-1650-x
50. Young AH (1984) Fractionation of starch. In: Starch: chemistry and technology. Academic Press, pp 249–283. https://doi.org/10.1016/B978-0-12-746270-7.50014-8
51. Dutta H, Paul SK, Kalita D, Mahanta CL (2011) Effect of acid concentration and treatment time on acid–alcohol modified jackfruit seed starch properties. Food Chem 128(2):284–291. https://doi.org/10.1016/j.foodchem.2011.03.016

52. Santha N, Sudha KG, Vijayakumari KP, Nayar VU, Moorthy AS (1990) Raman and infrared spectra of starch samples of sweet potato and cassava. J Chem Sci 102(5):705–712. https://doi.org/10.1007/BF03040801
53. Das RS, Agrawal YK (2011) Raman spectroscopy: recent advancements, techniques and applications. Vib Spectrosc 57(2):163–176. https://doi.org/10.1016/j.vibspec.2011.08.003
54. Ayala AP (2007) Polymorphism in drugs investigated by low wavenumber Raman scattering. Vib Spectrosc 45(2):112–116. https://doi.org/10.1016/j.vibspec.2007.06.004
55. Tomoda BT, Yassue-Cordeiro PH, Ernesto JV, Lopes PS, Péres LO, da Silva CF, de Moraes MA (2020) Characterization of biopolymer membranes and films: physicochemical, mechanical, barrier, and biological properties. Biopolym Membr Films. https://doi.org/10.1016/B978-0-12-818134-8.00003-1
56. Korsmeyer RW, Gurny R, Doelker E, Buri P, Peppas NA (1983) Mechanisms of solute release from porous hydrophilic polymers. Int J Pharm 15(1):25–35. https://doi.org/10.1016/0378-5173(83)90064-9

Publisher's Note